Environmental Science & Technology

pubs.acs.org/est

Article

New Mexico Permian Basin Measured Well Pad Methane Emissions Are a Factor of 5−9 Times Higher Than U.S. EPA Estimates

Anna M. Robertson, Rachel Edie, Robert A. Field, David Lyon, Renee McVay, Mark Omara, Daniel Zavala-Araiza, and Shane M. Murphy*

Cite This: *Environ. Sci. Technol.* 2020, 54, 13926−13934

Read Online

ACCESS | Metrics & More | Article Recommendations | Supporting Information

ABSTRACT: Methane emission fluxes were estimated for 71 oil and gas well pads in the western Permian Basin (Delaware Basin), using a mobile laboratory and an inverse Gaussian dispersion method (OTM 33A). Sites with emissions that were below detection limit (BDL) for OTM 33A were recorded and included in the sample. Average emission rate per site was estimated by bootstrapping and by maximum likelihood best log-normal fit. Sites had to be split into "complex" (sites with liquid storage tanks and/or compressors) and "simple" (sites with only wellheads/pump jacks/separators) categories to achieve acceptable log-normal fits. For complex sites, the log-normal fit depends heavily on the number of BDL sites included. As more BDL sites are included, the log-normal distribution fit to the data is falsely widened, overestimating the mean, highlighting the importance of correctly characterizing low end emissions when using log-normal fits. Basin-wide methane emission rates were estimated for the production sector of the New Mexico portion of the Permian and range from ∼520 000 tons per year, TPY (bootstrapping, 95% CI: 300 000−790 000) to ∼610 000 TPY (log-normal fit method, 95% CI: 330 000−1 000 000). These estimates are a factor of 5.5−9.0 times greater than EPA National Emission Inventory (NEI) estimates for the region.

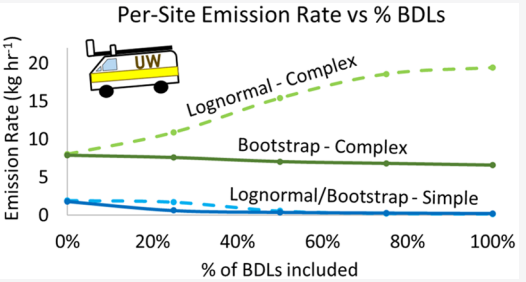

INTRODUCTION

Production of oil and natural gas in the United States has increased by over 200% and 150%, respectively, since 2005.[1] This boom has primarily been driven by the increased use of hydraulic fracturing combined with directional drilling technologies, allowing the extraction of fossil fuels from formations that were not economically feasible with prior drilling practices. Natural gas has been proposed as a bridge fuel toward a lower carbon economy with less carbon dioxide emissions than coal.[2] However, natural gas is primarily comprised of methane, a powerful greenhouse gas that has a global warming potential 86 times that of carbon dioxide over a 20 year period.[3] According to the most recent estimates from the U.S. Environmental Protection Agency (EPA), natural gas and petroleum systems are the largest anthropogenic source of methane emissions in the United States, accounting for 31% of man-made methane emissions. The production sector alone accounts for over 70% of emissions from natural gas and petroleum systems.[4]

A 2018 study by Alvarez et al.[5] used observations from several U.S. oil and gas (O&G) basins to determine that observed methane emissions are ∼60% higher than EPA emission estimates for the O&G sector, and observed emissions from the production sector alone are 2.2 times higher than EPA estimates, while a study by Howarth et al. suggests even larger underestimates of O&G sector emissions.[6] One explanation for this low bias in emission inventories is that they do not account for the "heavy-tail" or "fat-tail" of the emission distributions commonly observed in O&G basins. This "fat-tail" is caused by a small percentage of sites, a.k.a., "super-emitters," that disproportionately account for a large majority of emissions.[7−15] These high emissions can be the result of routine maintenance (e.g., liquid unloadings, well blowdowns) as well as equipment malfunctions that occur stochastically at any given site.[13] Due to the random nature of some of these larger leaks, they are difficult to account for in an emission inventory, but recent studies have demonstrated that using a more statistically robust method to estimate O&G emission distributions in emission inventories can successfully represent observed methane emissions.[5,7]

The Permian Basin is a highly active O&G basin spanning western Texas and southeastern New Mexico. Since 2007, oil and gas production have more than quadrupled and doubled in the basin, respectively. Currently, the basin has the highest oil production in the U.S., and gas production is second only to

Received: May 7, 2020
Revised: September 25, 2020
Accepted: October 2, 2020
Published: October 15, 2020

https://dx.doi.org/10.1021/acs.est.0c02927
Environ. Sci. Technol. 2020, 54, 13926−13934

the Marcellus Shale.[1] However, despite it being an important O&G basin, the current study is the first to report ground-based methane flux estimates in the Permian. Aircraft mass-balance flights have not yet successfully estimated a basin-wide emission rate due to the immense size of the basin[16] (~200 000 km^2), although current attempts are ongoing. This study examines the use of two different widely used statistical methods (bootstrapping and maximum likelihood log-normal fit) to estimate average emission rates that are then used to scale up facility-level methane emission rates to a basin-level estimate for well pad emissions.

MATERIALS AND METHODS

Mobile Laboratory Platform. Measurements were performed using the University of Wyoming Atmospheric Science Mobile Research Laboratory (Mobile Lab, Supporting Information (SI) Figure S1).[17−19] A mast extends out beyond the front bumper of the Mobile Lab and is 4 m off the ground to minimize wind interference/wake effects from the body of the vehicle or the ground. The mast houses meteorological instruments, including a 3D sonic anemometer, an AirMar GPS/2D wind sensor, and a 2D compact weather station. An inlet is also attached to the front of the mast which pulls air through approximately 7 m of $^1/_4$ in. Teflon tubing into instruments inside the lab at a rate of 7 LPM. During this project, a Picarro Cavity Ringdown Spectrometer (CRDS) was used to measure methane and water vapor mixing ratios (model G2204, modified by Picarro Inc. to sample at 2-Hz). The calibration of the Picarro was performed by sampling a NIST traceable (±1%) methane in ultrapure air mixture with a methane concentration of 2.576 ppm. The 2-Hz Picarro CRDS calibration fluctuated less than ±6 ppb over the course of the project and was always in agreement with the NIST standard.

Emission Flux Quantification. Methane emission fluxes were calculated using the Gaussian dispersion approach within the U.S. EPA's Other Test Method (OTM) 33A. This method has been described in detail in Brantley et al., Robertson et al., and EPA documentation.[19−21] The 1-sigma error for OTM 33A, verified by test releases performed under a wide variety of real-world conditions, is ±35% relative to a known release rate, which translates to an error of +54%/-26% for measurement of an unknown emission rate in the field.[22] Results using this method have been used in a measurement-based inventory to estimate emissions from other O&G production regions.[5,12] Briefly, this method uses rapid wind and methane mixing ratio measurements (~2 Hz) downwind of a site to calculate average methane enhancements for each wind direction over a minimum 20 min period. An advantage of OTM 33A is that it does not require site access from operators and therefore can limit the so-called "operator opt-in bias." During a measurement, as the plume wafts back and forth over the inlet, a plot of the time-averaged in-plume concentrations versus wind direction forms a Gaussian distribution.[23] The peak of a Gaussian fit to the data gives C_{peak} in eq 1 while the horizontal and vertical dispersion parameters (σ_y and σ_z) are determined from a lookup table based on distance from the source and atmospheric stability determined by variation in the horizontal and vertical winds. An emission flux (Q) is calculated by

$$Q = 2\pi \times \bar{U} \times \sigma_y \times \sigma_z \times C_{peak} \quad (1)$$

Where, $\bar{U}$ is the mean wind speed during the measurement (SI Section 1.2 gives further detail). The limit of detection (LOD)for the OTM 33A method was empirically determined to be 0.036 kg hr^{-1} (0.01 g/s).[20] While we have no empirical evidence that this is not a valid LOD at all distances, we agree that the LOD could vary with distance and meteorological conditions. Therefore, we ran sensitivity tests using varying detection limits (up to an order of magnitude greater, 0.36 kg hr^{-1}), but saw no significant effect on final results (detailed in SI Section 1.4).

Of the 111 measurements performed in the Permian Basin during this study, 47 yielded a quantified flux estimate with the OTM 33A technique and 29 sites were measured to be below detection limit (BDL) (number of measurements detailed further in SI Section 7.0). A measurement yields a flux estimate if it passes a series of data quality flags that are part of the OTM 33A analysis method, including flags for atmospheric stability, poor Gaussian fit of the emission plume, excessive wind variance, and others (see SI Section 1.3). An infrared optical gas imaging camera (FLIR GF300) was used at measurement sites to check for any large conflicting emission sources nearby (such as pipeline leaks) and to pinpoint emission sources on the well pad. A measurement may also be removed from the final data set during postprocessing if satellite imagery (from Google Earth) or analysis of the wind direction during the measurement suggest that there may have been an interfering source upwind.

Study Area. The Permian Basin is located in western Texas (TX) and southeastern New Mexico (NM). The Permian is broken into two main geologic basins: the Midland Basin on the eastern side, and the Delaware Basin (DB) on the western side, separated by the Central Basin Platform (SI Figure S3). For this study, 111 ground-based, facility-level methane emission measurements were collected in the DB during August 2018. Out of the 111 measurements, 71 were collected in NM and 40 were collected in TX. The sample number was lower in TX mostly due to lighter and more variable winds. Measurements were attempted in the Midland Basin, but due to lack of public road access the measurements were not successful. As of August 2018, there were approximately 144 000 active wells in the Permian Basin, roughly half (73 000) of which were located in the DB.[24]

Sampling Strategy. Due to the large size of the basin, a clustered random sampling strategy was implemented - clustered by production fields with the densest population of wells in the basin (SI Figure S4 and S5). This resulted in 8 original clusters, which were then stratified by production magnitude and age of wells to try to obtain a sample set that represented the large age and production range in the basin, including older/low producing wells, newer/high producing wells and those in-between. After a cluster was chosen for the day, we randomly selected sites based on wind direction and downwind road access. This strategy was chosen to minimize transit time between potential sites and to maximize sample size. As the field campaign progressed and the number of measurable sites in each of the original clusters began to dwindle (sites with good downwind road access for given winds had already been measured), 3 more clusters were added in areas that had a sufficient number of well pads that could be targeted. The end result was that the measurements collected in this study leaned more toward the newer/high producing end of the spectrum with an average age of 8 years, average gas production of 680 thousands of cubic feet per day (mcfd), and average oil production of 170 barrels per day (bpd). Whereas basin-average values for the DB in 2018 were 17 years, 160

https://dx.doi.org/10.1021/acs.est.0c02927
Environ. Sci. Technol. 2020, 54, 13926−13934

mcfd, and 41 bpd (SI Figure S6). Since newer/higher-producing wells tend to have higher methane emission rates than older/lower-producing wells, this sampling bias may have resulted in an overestimation of the average emission rate per well by up to 20% (details of this analysis are in SI Section 2.3). However, due to the low sample number and limited confidence in the robustness of the relationship between emissions and age/production, as well as the possibility that we may have underestimated the fat-tail (discussed more in the Section "Well Site Classification: Simple Vs Complex"), no correction factor was applied to the data.

Once a site was chosen for measurement, several transects downwind of the site were performed to locate the approximate center of the emission plume, where the Mobile Lab was then parked and the engine turned off to avoid exhaust interference. To check for interfering sources upwind several methods were employed either alone or in combination including performing transects upwind of the site when possible, using the FLIR camera to check pipeline junctions or other nearby sources, and using Google Earth imagery to ensure that there were no large sources nearby that we visually missed. If there was a large site directly upwind of the site of interest and we could not confirm that there were no conflicting emissions coming from that site then we did not measure. Wind direction and speed (10 Hz) and methane mixing ratios (2 Hz) were then measured for a period of at least 20 min to allow the plume to average out into a Gaussian. Sites where the Mobile Lab was clearly downwind, but where no emission plume was detected or emissions were below the detection limit for OTM 33A were recorded as below detection limit (BDL). All measurements were performed within 40−200 m of the source, with distance to source measured using a laser range finder.

Sites Below Detection Limit (BDL). In an effort to make the measurements as representative of the emission distribution in the DB as possible, sites where emissions were below the OTM 33A method's detection limit (0.036 kg hr^{-1}) were also recorded and will be referred to as below detection limit (BDL) sites. A site was recorded as BDL if, while sitting within 150 m downwind, maximum observed methane enhancements were below 50−100 ppb. This is the minimum enhancement distinguishable from background fluctuations that is necessary for an accurate flux estimate. Lofted plumes are a limitation of OTM 33A since measurements are performed from a ground-based vehicle at relatively close distances, so to verify that there were not plumes that were lofted over the inlet at these sites, each site was also verified to have no visible emissions using the FLIR camera from near the edge of the well pad. A site was also only recorded as BDL if the winds were consistent enough to ensure that we were directly downwind of all potential sources on the site. The lowest quantified emission with OTM 33A during this campaign was 0.068 kg hr^{-1}.

To include the BDL sites in the final statistics, first a "success fraction" was applied to the total number of BDL sites. The success fraction represents the fraction of total OTM measurements that passed data quality criteria and is applied to the number of BDL sites to include the same fraction of BDLs as OTM measurements. If this were not done the BDL sites would be statistically over-represented. Not including the success fraction decreases the final basin-level estimate by 5−7%. This success fraction was 72%, resulting in a total of 29 BDL sites counted in the final data set, 17 in NM, and 12 in TX. To estimate the emissions from these sites, values were chosen randomly with equal probability between 0 kg hr^{-1} and the method minimum detection limit (0.036 kg hr^{-1}). This approach likely underestimates the leakage rate assuming the BDLs actually follow the tail of the data set's log-normal distribution (which would result in the majority of BDL sites having an emission rate close to the LOD), but was chosen to be conservative. One caveat for the number of BDL sites is that the majority of them were measured for less than 5 min, and therefore some low frequency intermittent emissions could have been missed.

Well Site Classification: Simple Vs Complex. The oil and gas extracted at well pads needs to be separated (into oil, gas, and water) and sometimes further processed (e.g., dehydration of the gas), before it is stored on site or sent to a gathering pipeline. Typically, these processes occur at the well pad, where produced water and oil/condensate are sent to atmospheric storage tanks on site that flash gas (though some have controls that combust flashed emissions). However, the majority of sites in the DB have only wellheads or oil pump jacks on site with their production routed offsite to central gathering sites/tank batteries for processing and storage. These "simple" sites therefore have either no, or minimal, liquids storage or processing equipment on site, which have been shown to be the primary emission sources on well pads.[13,25] During analysis, it became apparent that these "simple" sites have a very different emission profile (median emission rate of 0.03 kg hr^{-1}) than sites with one or more compressors or liquids storage tanks on site (median emission rate of 2.6 kg hr^{-1}). Therefore, sites are broken into two categories for analysis: simple and complex sites. A complex site is defined in this study as any well pad with one or more oil/water storage tank(s) and/or compressor(s) on-site. All other sites are defined as simple, which includes well pads with only one or more wellhead(s), pump jack(s), and/or separator(s)/other simple equipment on-site. Of the 46 sites with flux estimates in NM, 30 were complex and 16 were simple. Of the 25 sites with flux estimates in TX, 17 were complex and 8 were simple.

This classification is especially important when estimating emission distributions and extrapolating facility-level emissions to a basin-level estimate. To extrapolate our measured emissions per site to a basin-level estimate for the NM portion of the DB, the number of wells in the basin during the month of measurement that were actively producing (August 2018:25 000 wells) was divided by the average number of wells per site (1.2) to get an approximate number of sites.[24] Wells that were listed as suspended/abandoned/etc. were not included in the scale-up. Then, the number of simple and complex well pads was calculated based on the results from human classification of satellite imagery (Airbus SPOT) that $\sim^2/_3$ of the well pads in the NM DB are "simple" with the remaining $^1/_3$ being "complex" (~97% of the sites had imagery from 2018 or 2019). This classification only includes well pads with at least one wellhead or pump jack on site. In our sample set, this ratio was reversed, with $\sim^2/_3$ of our sites that passed QA/QC being complex sites. A major focus of this field campaign was to capture the high-end of the emission distribution to avoid underestimating the fat-tail, which played into the sampling strategy. There was much less variation in emissions from simple sites (with a large majority of them being BDL) than complex sites so we began preferentially targeting the complex sites to better nail down their contribution to the emission distribution. Importantly, since we estimate average emissions for simple and complex sites

https://dx.doi.org/10.1021/acs.est.0c02927
Environ. Sci. Technol. 2020, 54, 13926−13934

separately, and then scale them up separately to a basin-level estimate, this complex-bias does not contribute to an overestimation of basin-level emissions. Also, although there are twice as many simple sites than complex sites in the basin, emissions from the complex sites dominate the emissions, representing 91% of total emissions.

A similar extrapolation for the TX portion of the basin was not performed due to the lower number of measurements on the TX side, and therefore less confidence in scaling up the data there, and because the classification of satellite imagery was only available for the NM side of the basin. There were only 13 successful site-level measurements (using OTM 33A) and 12 BDL sites from the TX side of the DB (0.05% of active wells in TX DB), as opposed to 29 successful site-level measurements and 17 BDLs on the NM side (0.18% of active wells in NM DB).

It is also important to note that although BDL sites were accounted for and included in the analysis, several sites with large methane enhancements that were either too spread out or too close to the road to sample due to the limitations of OTM 33A[17] were not accounted for/included in the analysis because we do not have approximate mass emission rates for them (similar sites with no emissions were recorded under the BDL category for complex sites). Often, the sites with large observed methane enhancements (15−20 PPM CH_4 from over 100 m away) were gathering facilities/tank batteries that only had tanks and processing equipment on-site but no wells or pump jacks and therefore were not quantified with OTM 33A, identified in the Google Earth analysis, or included in the basin-wide scale up. Since these sites do not have a well or pump jack on-site, they are also not listed in either the NM or TX production databases and there is no publicly available data on their throughput or which wells/pump jacks have production routed to them. Thus, these are likely a significant but currently unaccounted for emission source that requires further study to fully characterize the emissions in the basin. Furthermore, because we have production information for the simple sites but no information on where their production is sent, we may be underestimating their total emissions if their production is being sent to one of these unaccounted for central gathering facilities/tank batteries.

Statistical Techniques for Emission Estimation. Two common methods used for extrapolating facility- or well-level emissions data to a basin-wide estimate are bootstrapping and maximum likelihood best log-normal fit.[5,7,8,10,12,14,20,26−28] Each of these methods are a way to predict the average emission rate per well/site for a given data set. The average emission rate can then be multiplied by the total number of wells/sites to obtain a total emission rate for a basin or region. One of the objectives of this study is to compare the average emission rate calculated using these two methods and explore how and why they may differ.

Bootstrapping is a proven method used to approximate statistics (and their confidence intervals) of a population without assuming that the data come from any specific distribution. This method estimates statistics of the underlying population by resampling the measured data set (with replacement) a large number of times,[29] that is, "pulling the data up by its bootstraps". For this study, bootstrapping is used to estimate average emission rates per well pad (i.e., per site) and to investigate the production characteristics of different subsections of the DB. The bootstrapping method used in this study is described in detail in Robertson et al. 2017. Briefly, the error distribution for each measurement is first created using a normal distribution with the measured emission rate as the mean and the 1-sigma error estimate for OTM 33A (+54%/−26%)[22] as the standard deviation. The measurements with incorporated error are resampled with replacement 100 000 times, creating 100 000 new sample sets of the original sample size (e.g., n = 71 for all successful well pad measurements in the DB, n = 46 for NM, and n = 25 for TX). From these 100 000 sample sets one can calculate 100 000 estimates of the mean and the distribution of all the possible means can be used to determine the 95% CI.

Another popular method to estimate emissions from O&G basins is to assume the data follow a log-normal distribution and use the best log-normal fit to estimate population statistics.[5,7,12] It has been shown throughout U.S. O&G basins that a small fraction of sites account for a large fraction of the emissions resulting in a "fat-tail"/"heavy-tail" in the emission distribution. However, because this heavy-tail is caused by a small percentage of sites, it is difficult to make enough measurements to capture a significant fraction of these sites during a two- or three-week ground campaign.[30] Trying to accurately approximate the heavy-tail of the emissions distribution is critical because it drives the mean emission rate per well/site and therefore the extrapolation to a basin-level estimate. For this reason, studies have fit a log-normal distribution to measured emissions to estimate the heavy-tail. Notably, past studies of O&G basins have revealed that measured emission distributions often exhibit even more extreme distributions than a log-normal fit.[9] For this study, Matlab's (version R2018b) log-normal fitting routine, based on maximum likelihood estimation (MLE), was used to evaluate the best log-normal fit to the emission distribution, fitting complex and simple sites as two separate distributions. The lognormality of the data sets is explored more in the Results and Discussion.

Converting Gas Production to Methane Production. Monthly oil and gas production data for measured sites were obtained from the DrillingInfo database.[24] The monthly natural gas production (NGP) rates are converted from thousands of cubic feet of natural gas per month (mcf/mo) to kilograms of gross methane produced (GMP) per hour (kg hr^{-1}) using eq 2:

$$\mathrm{GMP}\left(\frac{\mathrm{kg}}{h}\right) = \mathrm{NGP}\left(\frac{\mathrm{mcf}}{\mathrm{mo}}\right) \times \left[\frac{\left(1000\frac{\mathrm{ft}^3}{\mathrm{mcf}}\right) \times \left(1.19804\frac{\mathrm{molgas}}{\mathrm{ft}^3}\right) \times \left(xx\frac{\mathrm{molCH_4}}{\mathrm{molgas}}\right) \times \left(0.01604\frac{\mathrm{kg}}{\mathrm{molCH_4}}\right)}{(\#\mathrm{days/mo})(24\mathrm{h/day})}\right] \quad (2)$$

The Permian Basin is a wet gas basin, and publicly available composition data for natural gas produced in the DB is sparse but existing reports cite a methane content (mol CH_4/mol gas) of 60−75%.[31,32] For this study, methane content for each site was randomly chosen from a normal distribution centered on 70%, with 95% of values falling between 64 and 76%. This

https://dx.doi.org/10.1021/acs.est.0c02927
Environ. Sci. Technol. 2020, 54, 13926−13934

was done to be as robust as possible with any potential errors involved in the calculation, but pulling random values versus using the same methane content (e.g., 70%) for each measurement had a negligible effect on the final results.

TNMA, ENMA, and Oil Fraction. A throughput-normalized mass average (TNMA) emission, often referred to as the average fraction of methane produced that was emitted to the atmosphere, is calculated following eq 3:

$$\mathrm{TNMA}(\%) = \frac{\sum \mathrm{MMER}\left(\frac{\mathrm{kg}}{\mathrm{h}}\right)}{\sum \mathrm{GMP}\left(\frac{\mathrm{kg}}{\mathrm{h}}\right)} \times 100 \tag{3}$$

Where MMER is the measured methane emission rate (either using OTM 33A or estimated for BDLs), and GMP is the gross methane produced as defined in eq 2. As opposed to separate throughput-normalized emissions for each facility, TNMA represents a basin-average throughput-normalized emission rate.

As mentioned earlier, the DB also produces considerable quantities of oil and therefore all methane emissions from a site cannot be attributed entirely to natural gas production. Average oil fraction, that is, the fraction of total energy production at the site that can be attributed to oil, is calculated as follows:

$$\text{average oil fraction} = \frac{\sum \mathrm{OP}\left(\frac{\mathrm{bbl}}{\mathrm{d}}\right)}{\sum \mathrm{totalBOE}\left(\frac{\mathrm{bbl}}{\mathrm{d}}\right)} = \frac{\sum \mathrm{OP}\left(\frac{\mathrm{bbl}}{\mathrm{d}}\right)}{\sum \left[\mathrm{OP}\left(\frac{\mathrm{bbl}}{\mathrm{d}}\right) + \mathrm{OEGP}\left(\frac{\mathrm{bbl}}{\mathrm{d}}\right)\right]} \tag{4}$$

Where OP is oil production, OEGP is the oil equivalent gas production, and BOE is the barrels of oil equivalent. Gas production is converted to equivalent barrels of oil (OEGP) using the Society of Petroleum Engineer's (SPE) conversion ratio of 5.8 mcf of gas = 1 BOE.[33] Since some sites primarily produce oil with some associated gas, an energy-normalized mass average (ENMA), or the fraction of energy produced (oil plus gas) that is emitted to the atmosphere as methane, is calculated following the same method as Robertson et al. 2017:[19]

$$\mathrm{ENMA}(\%) = \frac{\sum \mathrm{MEER}\left(\frac{\mathrm{Btu}}{\mathrm{d}}\right)}{\sum \mathrm{EEP}\left(\frac{\mathrm{Btu}}{\mathrm{d}}\right)} \times 100 \tag{5}$$

where MEER is the measured energy emission rate, and EEP is the equivalent energy production. Total energy production (oil plus gas) was converted to units of Btu using the standard values from the SPE of 5.8×10^6 Btu per barrel of oil and 1×10^6 Btu per mcf of gas.[34]

RESULTS AND DISCUSSION

Raw Emissions Distribution. Plotting the cumulative emission distribution for measurements of individual well pads using OTM 33A and estimated emissions for BDLs reveals that, similar to results from other basins,[7−12] the emission distribution in the DB exhibits a skewed, or heavy-tailed, distribution (SI Figure S8). In the DB, the top 15% of emitters had emissions of at least 7 kg hr^{-1} and accounted for over 70% of total emissions. The top 5% of emitters had emissions of at least 20 kg hr^{-1} and accounted for over 30% of total emissions, both in NM and TX. The lognormality of the data set is explored further in the "Per-Site Emission Rate" section.

Bootstrapped Mass Emission Rate, TNMA, Oil Fraction, and ENMA. The results from bootstrapping the emission and production data in the DB are shown in Figure 1

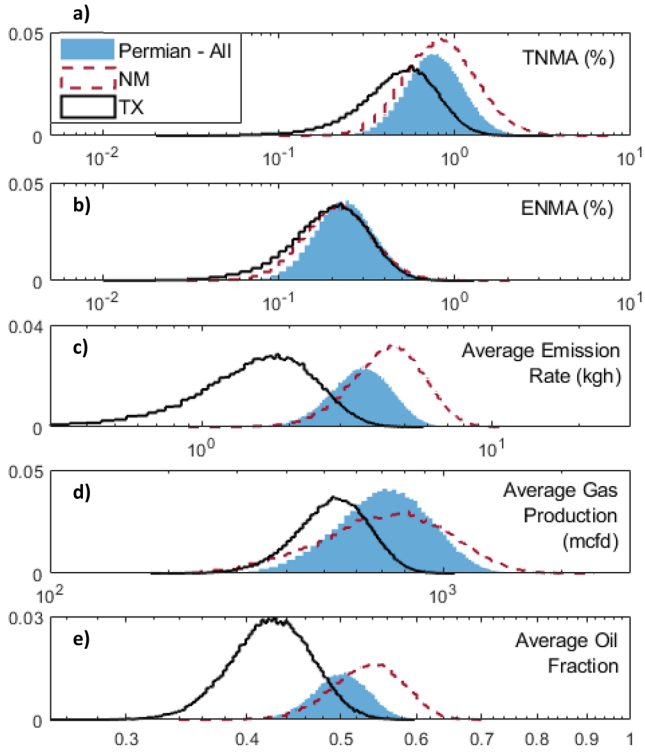

Figure 1. Probability density functions of average emission rates derived by bootstrapping measurements. Panels show all well pads in the DB (blue, filled in), well pads in the NM portion of the DB (red dashed line), and well pads in the TX portion of the DB (black solid line). Panels are (a) throughput-normalized mass average (TNMA, %), (b) energy-normalized mass average (ENMA, %), (c) average mass emission rate per facility (kg hr^{-1}), and (d) average gas production per facility (mcfd), and e) average oil fraction per facility.

and Table 1. Measurements performed in NM and TX are separated to compare differences at the state level. Notably, there were only 13 OTM and 12 BDL measurements on the TX side versus 29 OTM and 17 BDL measurements on the NM side (SI Section 7.0), so the results from TX may be skewed by the lower sample size. Statistics are also presented combining measurements from both states, represented as "DB" in Figure 1 and Table 1. To provide context for the current work, results from the DB are compared to statistics from other US basins calculated using the same methods (past work refers to Robertson et al. 2017[19]). In these previous studies there was never a statistical reason to separate sites into simple and complex sites. The central estimate for mean TNMA emission rate (Figure 1a) for well pads in the DB is 0.88% (0.42−1.83, 95% CI), which puts the basin midway between previous well pad TNMA emission estimates for the Upper Green River (UGR) Basin and Fayetteville (FV) gas play of 0.1−0.2% and the Denver-Julesburg (DJ) and Uinta Basins of 2−3% (previous estimates shown in SI Figure S9). The central estimate of mean facility-level mass emission rates (Figure 1c) in the DB is 3.8 kg hr^{-1} of methane (2.2−5.7, 95% CI), which is comparable to the average emission rate measured in the Uinta Basin (3.7 kg hr^{-1}), which is the highest we observed from previously measured basins. The

https://dx.doi.org/10.1021/acs.est.0c02927
Environ. Sci. Technol. 2020, 54, 13926−13934

Table 1. Summary of Central Estimates for Facility-Level Mean Emissions (Bootstrapped Distributions Shown in Figure 1)

portion of basin	mean TNMA—% (95% CI)	mean ENMA—% (95% CI)	mean mass emission rate—kg hr^{-1} (95% CI)	mean gas production—mcfd (95% CI)	mean oil fraction (95% CI)
DB	0.89 (0.42−1.83)	0.26 (0.12−0.56)	3.76 (2.24−5.71)	762 (435−1210)	0.50 (0.44−0.57)
NM	1.03 (0.42−2.69)	0.26 (0.11−0.66)	4.74 (2.58−7.61)	818 (377−1470)	0.54 (0.45−0.62)
TX	0.61 (0.22−1.30)	0.25 (0.09−0.55)	1.89 (0.70−3.52)	551 (352−786)	0.43 (0.35−0.51)

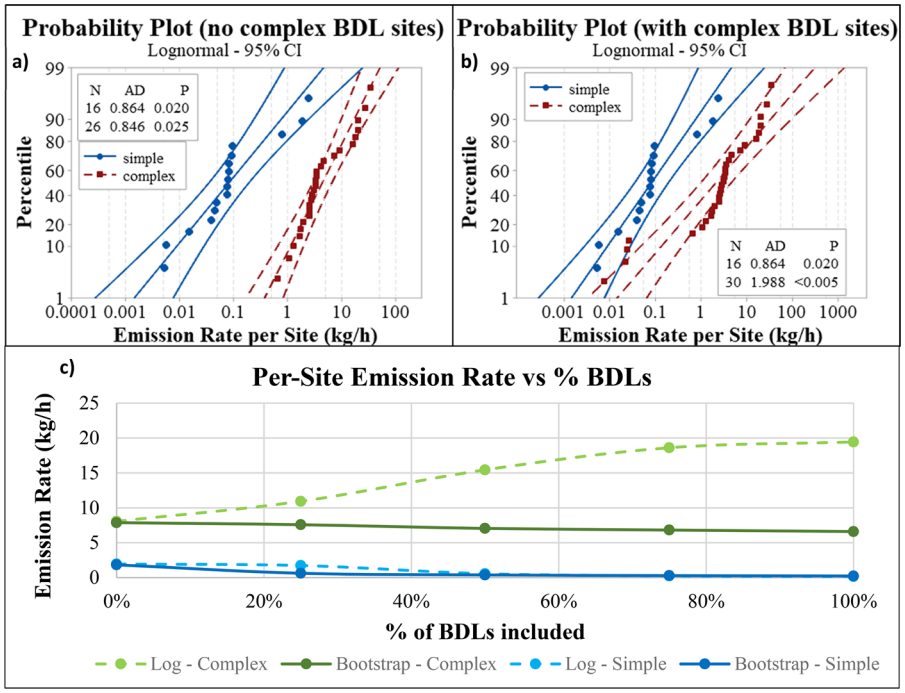

Figure 2. Top two panels show probability plots (emission rate versus percentile) to illustrate how well the measured emission rate data follow a log-normal fit with (a) no complex BDL sites included, and (b) with complex BDL sites included. The distribution for the simple sites is the same in panels a and b (both include BDL sites). The complex BDL sites in panel b are the four data points below 0.1 kgh^{-1}, denoted here as kg/h. Blue circle markers are simple sites and red squares are complex sites. The central lines show the best log-normal fit with outside lines showing 95% confidence bounds (solid lines for the simple site distribution, dashed lines for the complex sites distribution). In the legend, N is the sample size, AD is the Anderson-Darling statistic, and P is the corresponding *p*-value, with the values for simple sites on the top row and the values for complex sites on the bottom row. The bottom panel shows estimated per-site emission rate (kgh) for wells measured in the NM portion of the DB, estimated with both the bootstrapping and log-normal methods using different fractions of the total measured number of below detection limit (BDL) sites. Numbers of BDLs are plotted at increments of 25%, from 0% (0 BDLs) to 100% (28 BDLs).

distributions of measured mass emission rates and TNMA are broken down further into simple and complex sites for both NM and TX in SI Figure S10. Average gas production per well pad (Figure 1d) is approximately 820 mcfd in NM, similar to the relatively high production rate seen in FV and UGR, and about 50% higher than the average production observed at the TX well pads (550 mcfd). Well counts for NM and TX well pads were similar with an average of 1.2 and 1.1 wells per site, respectively. Wells in the DB overall have a much higher oil fraction (Figure 1e) than has been observed in other basins with a median value of 0.50 (0.44−0.57, 95% CI). For reference, the DJ Basin in Colorado, which also produces a considerable amount of oil along with its gas production, has an oil fraction of 0.2−0.3. Accordingly, emission rates were also normalized by total energy production (ENMA). The median ENMA (Figure 1b) for the DB is 0.29% (0.14−0.60%, 95% CI).

Per-Site Emission Rate: Lognormal Versus Bootstrapping. To scale measured methane mass emission rates up to a basin-level estimate for the NM portion of the basin, first a per-site emission rate was estimated separately for complex and simple sites using two different methods: (1) bootstrapping and (2) best log-normal fit. Then, a basin-level estimate was calculated using the number of actively producing simple and complex sites on the NM side of the DB at the time of measurement and their respective average emission rates per site. In August 2018, there were approximately 21 000 active sites in the DB.[24] Using the estimate from the manual counting of satellite imagery that ∼66% of well pads in the basin were simple and ∼33% were complex results in approximately 14 000 simple sites and 7000 complex sites. For the bootstrap method, the per-site emission rate was estimated to be 0.37 kg CH_4 $site^{-1}$ hr^{-1} (0.03−0.87, 95% CI) for simple sites, and 7.5 kg CH_4 $site^{-1}$ hr^{-1} (4.1−12, 95% CI) for complex sites. Resulting in a basin-level estimate of 520 000 tons per year, TPY (300 000−790 000, 95% CI).

Figure 2 illustrates how well the measured simple and complex sites follow a log-normal distribution. When fitting a log-normal distribution to the simple site emission rates (with estimates for the 13 simple BDL sites included), the resulting *p*-value is 0.02 and the Anderson-Darling (AD) statistic is moderate (0.9), indicating that the null hypothesis that the data come from a log-normal distribution cannot be rejected at the α = 0.01 level and that the log-normal assumption is

https://dx.doi.org/10.1021/acs.est.0c02927
Environ. Sci. Technol. 2020, 54, 13926−13934

reasonable for estimating an average emission rate. On the other hand, trying to fit a log-normal distribution to the complex sites (with the four complex BDL sites included), results in a p-value $\ll$0.01 and a relatively high AD statistic of 2.0 (Figure 2b), indicating that the null hypothesis is rejected and the data do not follow a log-normal distribution. The probability plot (Figure 2b) also suggests that there is a very low probability that the complex BDL sites actually belong on the same distribution as the rest of the complex sites since they are either right on or just outside of the 95% confidence bounds. This may indicate that the complex sites are more likely to have emissions above the detection limit. Undoubtedly, the complex BDL sites are more likely than the simple sites to have intermittent emissions that may have been missed because of the large number of operations occurring on site. The probability plots in Figure 2 also reveal that if the complex BDL sites are included (Figure 2b), it widens the log-normal distribution fit to the data (compared to Figure 2a). Therefore, including these low emitting sites actually increases the mean emission rate for complex sites when estimated using a log-normal distribution. This behavior is explored further in SI Table S1. If the complex BDL sites are excluded from the complex site distribution (Figure 2a), the p-value and AD statistic are similar to those for the simple site distribution, indicating that assuming a log-normal distribution for the emission rates from complex sites is more valid if the complex BDL sites are not included.

As a result, the following analysis will present results using three different approaches: (1) the four complex BDL sites are excluded from the log-normal fit to the complex sites, (2) the four complex BDL sites are excluded from the fit but are factored into the final basin-level emission estimate by assuming the same ratio of BDL complex sites (4/30 = 13%) while using 0.036 kg hr^{-1} as their emission rate, and (3) the four complex BDL sites are included in the log-normal fit (with BDL values chosen randomly between 0.01 and 0.036 kg hr^{-1} to match the BDL estimation for simple sites). Note, the third method, as discussed above, results in an invalid log-normal fit but is included here for illustrative purposes.

Using the first approach, the best log-normal fit resulted in per-site emission estimates of 0.43 kg CH_4 $site^{-1}$ hr^{-1} for simple sites (0.03−1.93, 95% CI) and 8.8 kg CH_4 $site^{-1}$ hr^{-1} for complex sites (4.6−15, 95% CI). The log-normal parameters for the fit to simple sites are $\mu = -3.1$, $\sigma = 1.8$, mode = 0.0016; and for the complex sites: $\mu = 1.5$, $\sigma = 1.1$, mode = 1.4. This results in a basin-level emission estimate of 610 000 TPY (330 000−1 000 000, 95% CI). The log-normal method results in a larger emission estimate than the bootstrapping method (520 000 TPY) since it includes a larger fat-tail in its estimated emission distribution. The second approach results in the same per-site emission rates and log-normal parameters as the first approach, but factoring the fraction of BDL sites into the basin-level roll-up results in a smaller basin-level estimate of 540 000 TPY (290 000−940 000, 95% CI). The third approach results in a similar average per-site emission rate for the simple sites of 0.47 kg CH_4 hr^{-1} $site^{-1}$ (0.03−1.7, 95% CI), but a much higher emission rate for complex sites since the log-normal fit is incorrectly widened with the inclusion of the BDL sites: 29 kg CH_4 hr^{-1} $site^{-1}$ (7.9−56, 95% CI). Using this approach results in a basin-level estimate of 1 900 000 TPY (540 000−3 600 000, 95% CI).

The sensitivity of the log-normal fit to the number and emission estimates chosen for the BDLs is explored further in Figure 2c and SI Section 6.0. In summary, as an increasing number of BDLs are included in the complex site emission distribution, the best log-normal fit to the data increasingly widens, resulting in larger and larger average emission rates and an increasing divergence from bootstrapping estimates. Therefore, although log-normal fits have been widely used to better characterize the heavy-tail of emission distributions in O&G basins to avoid underestimating total emissions, it is also important to ensure the low end of emissions is representative of the population so that average emission rates are not overestimated when using this approach.

Comparison to EPA Emission Inventories. Since production, and consequently emissions, has changed so drastically in the Permian in the last 5 years, comparisons were only made to the most recently available emission inventories, the EPA's Greenhouse Gas Reporting Program (GHGRP) and National Emission Inventory (NEI). All operators that emit more than 25 000 tons (t) CO_2-equivalent (CO_2e) per year must report their emissions through the GHGRP. However, although the EPA states that the GHGRP accounts for 85−90% of total U.S. emissions compared to their greenhouse gas inventory (GHGI), the majority of the O&G well pads in the basin likely are not included in the total since they do not meet the 25 000 t CO_2e annual emission threshold. The emission estimate for the O&G production sector (i.e., no gathering, boosting, or transmission) is only reported at the basin-level in the GHGRP. For the Permian Basin in 2018, 68 operators reported their annual production sector emissions for a total of ∼216 000 TPY CH_4. To estimate emissions from just the NM portion of the basin so that our measurements could be more directly compared, total emissions from the Permian were divided based on the fraction of total basin production from NM in 2018 (∼21%).[24] Taking 21% of the total results in approximately 45 000 TPY of methane from the NM portion of the basin. Comparing this value to our basin-level estimate of 520 000 TPY (using the bootstrapping method) to 610 000 TPY (using the first approach to the log-normal method), suggests that the inventory is over an order of magnitude low for this region.

To generate an estimate from the EPA's NEI 2017 data, the 2017 NEI Production Oil and Gas Tool was used (v1_1). For all O&G production activities in the NM portion of the basin, the NEI 2017 estimates total methane emissions of 91 000 TPY. Excluding truck loading and blowdown emissions from the NEI 2017 estimate, which were not included in our basin-level scale-up, yields a methane emission rate of 67 000 TPY (a factor of 7.8−9.0 times lower than our estimate). However, as mentioned previously, the Permian Basin reported large increases in oil and gas production from 2017 to 2018, with oil production increasing by ∼40% and gas production by ∼30%.[35] Because NEI 2018 emissions are not available, we scale the NEI emission estimates by the larger change in production (40%), yielding total methane emissions of 127 000 TPY, and 94 000 TPY if truck loading and blowdown emissions are excluded. Suggesting that the NEI is underestimating methane emissions by a factor of 5.5−6.5.

Comparison to Other Basins. To put methane emissions from the Permian into perspective, estimated basin-wide emissions from only well pads in just the NM portion of the basin (520 000−610 000 TPY CH_4) exceed total basin-wide emissions (i.e., all O&G operations) estimated using aircraft

https://dx.doi.org/10.1021/acs.est.0c02927
Environ. Sci. Technol. 2020, 54, 13926−13934

mass balance techniques in almost every other O&G basin in the U.S. (Alvarez et al. (2018)[5] demonstrated that bottom-up estimates using OTM 33A give statistically similar results to aircraft mass balance techniques). The one exception is the Eagle Ford Shale region in southern TX with total emissions estimated to be 730 000 (±190 000) TPY CH_4.[16] The same study that measured the Eagle Ford (Peischl et al. 2018) also estimated basin-wide methane emissions from O&G operations in several other U.S. basins and reported (TPY CH_4): 250 000 (±61 000) in the Bakken; 370 000 (±160 000) in Haynesville; and 400 000 (±260 000) in the Barnett. Basin-wide methane emissions for the Denver-Julesburg Basin were estimated in two separate studies (2012 and 2015) to be 160 000 (±70 000) − 170 000 (±60 000) TPY CH_4.[16,36] Lastly, Karion et al. (2013) estimated emissions from the Uinta Basin to be 480 000 (±130 000) TPY CH_4.

Future Studies. As this is the first ground-based study of the PB, and only the western portion of the PB, many questions remain and further research is needed to fully characterize emissions in the basin. One important question is how methane emissions in the eastern portion of the basin (Midland Basin) compare to those measured in the DB. Another important question is what fraction of total methane emissions in the basin are contributed by well pad emissions? Comparing our results to a recent satellite study by Zhang et al. (2020) which reported total methane emissions from O&G operations in the DB to be 1.7×10^6 TPY,[37] suggests this ratio may be 31−35%. There are several other significant emission sources in the basin not measured in this study, including but not limited to, gathering facilities/tank batteries, compressor stations, leaks along gathering pipelines (including in-line compressors), processing plants, and emissions from unlit or inefficient flare stacks. Emissions from gathering facilities/tank batteries would be particularly informative in trying to gain more information about total emissions from the simple sites measured in this study. Lastly, the measurement of older/low-producing wells should be a priority for future studies to gain a better understanding of the relationship between emissions and age/production of wells in the basin.

■ ASSOCIATED CONTENT

Supporting Information

The Supporting Information is available free of charge at https://pubs.acs.org/doi/10.1021/acs.est.0c02927.

> Details of the OTM 33A methodology; study region and sampling strategy; comparison to previous measurements and subcategories of data presented here; further analysis of the log-normal fit method used; and additional data for all measurements (PDF)

■ AUTHOR INFORMATION

Corresponding Author

Shane M. Murphy − *Department of Atmospheric Science, University of Wyoming, Wyoming 82071, United States;* orcid.org/0000-0002-6415-2607; Phone: 1-307-766-6408; Email: Shane.Murphy@uwyo.edu

Authors

Anna M. Robertson − *Department of Atmospheric Science, University of Wyoming, Wyoming 82071, United States*

Rachel Edie − *Department of Atmospheric Science, University of Wyoming, Wyoming 82071, United States;* orcid.org/0000-0001-7959-4232

Robert A. Field − *Department of Atmospheric Science, University of Wyoming, Wyoming 82071, United States*

David Lyon − *Environmental Defense Fund, Austin, Texas 78701, United States*

Renee McVay − *Environmental Defense Fund, Austin, Texas 78701, United States*

Mark Omara − *Environmental Defense Fund, Austin, Texas 78701, United States;* orcid.org/0000-0002-8933-1927

Daniel Zavala-Araiza − *Environmental Defense Fund, Austin, Texas 78701, United States;* orcid.org/0000-0002-8394-5725

Complete contact information is available at: https://pubs.acs.org/10.1021/acs.est.0c02927

Notes

The authors declare no competing financial interest.

■ ACKNOWLEDGMENTS

We acknowledge the Environmental Defense Fund (EDF) for providing funding and guidance on this work. We also acknowledge the University of Wyoming's School of Energy Resources who provided funding for the equipment used during this project and for funding of the Center of Excellence in Air Quality. We also thank the University of Wyoming Department of Atmospheric Science team of engineers for keeping our mobile laboratory running smoothly.

■ REFERENCES

(1) U.S. Energy Information Administration. No Title https://www.eia.gov/.

(2) Hausfather, Z. Bounding the Climate Viability of Natural Gas as a Bridge Fuel to Displace Coal. *Energy Policy* **2015**, *86*, 286−294.

(3) Myhre, G.; Shindell, D.; Bre′on, F.-M.; Collins, W.; Fuglestvedt, J. .; Huang, J.; Koch, D.; Lamarque, J.-F.; Lee, D.; Mendoza, B.; Nakajima, T; Robock, A.; Stephens, G.; Takemura, T.; Zhan, H. *Anthropogenic and Natural Radiative Forcing. In Climate Change 2013: The Physical Science Basis*; Contribution of Working Group I to the Fifth Assessment Report of the Intergovernmental Panel on Climate Change, 2013; pp 659−740 DOI: 10.1017/CBO9781107415324.018.

(4) U.S. Environmental Protection Agency. *Inventory of U.S. Greenhouse Gas Emissions and Sinks: 1990−2014*, 2016.

(5) Alvarez, R. A.; Zavala-Araiza, D.; Lyon, D. R.; Allen, D. T.; Barkley, Z. R.; Brandt, A. R.; Davis, K. J.; Herndon, S. C.; Jacob, D. J.; Karion, A.; Kort, E. A. Assessment of Methane Emissions from the U.S. Oil and Gas Supply Chain. *Science* **2018**, *361*, 186−188.

(6) Howarth, R. W. Ideas and Perspectives: Is Shale Gas a Major Driver of Recent Increase in Global Atmospheric Methane? *Biogeosciences* **2019**, *16* (15), 3033−3046.

(7) Zavala-Araiza, D.; Lyon, D. R.; Alvarez, R. A.; Davis, K. J.; Harriss, R.; Herndon, S. C.; Karion, A.; Kort, E. A.; Lamb, B. K.; Lan, X.; Marchese, A. J. Reconciling Divergent Estimates of Oil and Gas Methane Emissions. *Proc. Natl. Acad. Sci. U. S. A.* **2015**, *112* (51), 15597−15602.

(8) Rella, C. W.; Tsai, T. R.; Botkin, C. G.; Crosson, E. R.; Steele, D. Measuring Emissions from Oil and Natural Gas Well Pads Using the Mobile Flux Plane Technique. *Environ. Sci. Technol.* **2015**, *49*, 4742−4748.

(9) Brandt, A. R.; Heath, G. A.; Cooley, D. Methane Leaks from Natural Gas Systems Follow Extreme Distributions. *Environ. Sci. Technol.* **2016**, *50*, 12512−12520.

(10) Omara, M.; Sullivan, M. R.; Li, X.; Subramanian, R.; Robinson, A. L.; Presto, A. A. Methane Emissions from Conventional and

Unconventional Natural Gas Production Sites in the Marcellus Shale Basin. *Environ. Sci. Technol.* **2016**, *50* (4), 2099−2107.
(11) Bell, C. S.; Vaughn, T. L.; Zimmerle, D.; Herndon, S. C.; Yacovitch, T. I.; Heath, G. A.; Petron, G.; Edie, R.; Field, R. A.; Murphy, S. M.; Robertson, A. M. Comparison of Methane Emission Estimates from Multiple Measurement Techniques at Natural Gas Production Pads. *Elementa Science of the Anthropocene* **2017**, *5* (79).79
(12) Omara, M.; Zimmerman, N.; Sullivan, M. R.; Li, X.; Ellis, A.; Cesa, R.; Subramanian, R.; Presto, A. A.; Robinson, A. L. Methane Emissions from Natural Gas Production Sites in the United States: Data Synthesis and National Estimate. *Environ. Sci. Technol.* **2018**, *52* (21), 12915−12925.
(13) Lyon, D. R.; Alvarez, R. A.; Zavala-Araiza, D.; Brandt, A. R.; Jackson, R. B.; Hamburg, S. P. Aerial Surveys of Elevated Hydrocarbon Emissions from Oil and Gas Production Sites. *Environ. Sci. Technol.* **2016**, *50*, 4877−4886.
(14) Zavala-Araiza, D.; Alvarez, R. A.; Lyon, D. R.; Allen, D. T.; Marchese, A. J.; Zimmerle, D. J.; Hamburg, S. P. Super-Emitters in Natural Gas Infrastructure Are Caused by Abnormal Process Conditions. *Nat. Commun.* **2017**, *8* (1), 1−10.
(15) Allen, D. T. Emissions from Oil and Gas Operations in the United States and Their Air Quality Implications. *J. Air Waste Manage. Assoc.* **2016**, *66* (6), 549−575.
(16) Peischl, J.; Eilerman, S. J.; Neuman, J. A.; Aikin, K. C.; de Gouw, J.; Gilman, J. B.; Herndon, S. C.; Nadkarni, R.; Trainer, M.; Warneke, C.; Ryerson, T. B. Quantifying Methane and Ethane Emissions to the Atmosphere From Central and Western U.S. Oil and Natural Gas Production Regions. *J. Geophys. Res. Atmos.* **2018**, *123*, 7725−7740.
(17) Edie, R.; Robertson, A. M.; Field, R. A.; Soltis, J.; Snare, D. A.; Zimmerle, D.; Bell, C. S.; Vaughn, T. L.; Murphy, S. M. Constraining the Accuracy of Flux Estimates Using OTM 33A. *Atmos. Meas. Tech.* **2020**, *13* (1), 341−353.
(18) Edie, R.; Robertson, A. M.; Soltis, J.; Field, R. A.; Snare, D.; Burkhart, M. D.; Murphy, S. M. Off-Site Flux Estimates of Volatile Organic Compounds from Oil and Gas Production Facilities Using Fast-Response Instrumentation. *Environ. Sci. Technol.* **2020**, *54*, 1385−1394.
(19) Robertson, A. M.; Edie, R.; Snare, D.; Soltis, J.; Field, R. A.; Burkhart, M. D.; Bell, C. S.; Zimmerle, D.; Murphy, S. M. Variation in Methane Emission Rates from Well Pads in Four Oil and Gas Basins with Contrasting Production Volumes and Compositions. *Environ. Sci. Technol.* **2017**, *51*, 8832−8840.
(20) Brantley, H. L.; Thoma, E. D.; Squier, W. C.; Guven, B. B.; Lyon, D. Assessment of Methane Emissions from Oil and Gas Production Pads Using Mobile Measurements. *Environ. Sci. Technol.* **2014**, *48* (24), 14508−14515.
(21) U.S. Environmental Protection Agency. Other Test Method (OTM) 33 and 33A Geospatial Measurement of Air Pollution-Remote Emissions Quantification Direct Assessment (GMAP-REQ-DA). http://www.epa.gov/%0Attn/emc/prelim.html.
(22) Edie, R.; Robertson, A.; Field, R.; Soltis, J.; Snare, D.; Zimmerle, D.; Bell, C.; Vaughn, T.; Murphy, S. Constraining the Accuracy of Flux Estimates Using OTM 33A. *Atmos. Meas. Tech.* **2020**, *13*, 341−353.
(23) Turner, D. B. Workbook of Atmospheric Dispersion Estimates. Publication No. 999-AP-26. 1969.
(24) DrillingInfo DI Desktop. No Title enverus.com.
(25) Allen, D. T. Emissions from Oil and Gas Operations in the United States and Their Air Quality Implications. *J. Air Waste Manage. Assoc.* **2016**, *66* (6), 549−575.
(26) Brantley, H. L.; Thoma, E. D.; Eisele, A. P. Assessment of VOC and HAP Emissions from Oil and Natural Gas Well Pads Using Mobile Remote and Onsite Direct Measurements. *J. Air Waste Manage. Assoc.* **2015**, *65* (9), 1072−1082.
(27) Allen, D. T.; Pacsi, A. P.; Sullivan, D. W.; Zavala-araiza, D.; Harrison, M.; Keen, K.; Fraser, M. P.; Hill, a D.; Sawyer, R. F.; Seinfeld, J. H. Methane Emissions from Process Equipment at Natural Gas Production Sites in the United States: Pneumatic Controllers. *Environ. Sci. Technol.* **2015**, *49* (1), 630−640.
(28) Yacovitch, T. I.; Daube, C.; Vaughn, T. L.; Bell, C. S.; Roscioli, J. R.; Knighton, W. B.; Nelson, D. D.; Zimmerle, D.; Pétron, G.; Herndon, S. C. Natural Gas Facility Methane Emissions: Measurements by Tracer Flux Ratio in Two US Natural Gas Producing Basins. *Elementa Science of the Anthropocene* **2017**, *5* (69).69
(29) Efron, B.; Tibshirani, R. Bootstrap Methods for Standard Errors, Confidence Intervals, and Other Measures of Statistical Accuracy. *Stat. Sci.* **1986**, *1* (1), 54−77.
(30) Caulton, D. R.; Lu, J. M.; Lane, H. M.; Buchholz, B.; Fitts, J. P.; Golston, L. M.; Guo, X.; Li, Q.; McSpiritt, J.; Pan, D.; Wendt, L. Importance of Superemitter Natural Gas Well Pads in the Marcellus Shale. *Environ. Sci. Technol.* **2019**, *53*, 4747−4754.
(31) Howard, T.; Ferrara, T. W.; Townsend-Small, A. Sensor Transition Failure in the High Flow Sampler: Implications for Methane Emission Inventories of Natural Gas Infrastructure. *J. Air Waste Manage. Assoc.* **2015**, *65* (7), 856−862.
(32) Broadhead, R. F.; Mansell, M.; Jones, G. *Carbon Dioxide in New Mexico: Geologic Distribution of Natural Occurrences*, Report No. 514; New Mexico Bureau of Geology and Mineral Resources A Division of New Mexico Tech: Socorro, NM, 2009.
(33) Society of Petroleum Engineers. Guidelines for the evaluation of petroleum reserves and resources http://www.spe.org/%0Aindustry/docs/GuidelinesEvaluationReservesResources_2001.pdf.
(34) Society of Petroleum Engineers. Unit Conversion Factors www.spe.org/industry/unit-conversion-factors.php.
(35) New Mexico Oil Conservation Division. http://www.emnrd.state.nm.us/ocd/.
(36) Petron, G.; Karion, A.; Sweeney, C.; Miller, B. R.; Montzka, S. A.; Frost, G. J.; Trainer, M.; Tans, P.; Andrews, A.; Kofler, J.; Helmig, D. A New Look at Methane and Nonmethane Hydrocarbon Emissions from Oil and Natural Gas Operations in the Colorado Denver-Julesburg Basin. *J. Geophys. Res.: Atmos.* **2014**, *119*, 6836−6852.
(37) Zhang, Y.; Gautam, R.; Pandey, S.; Omara, M.; Maasakkers, J. D.; Sadavarte, P.; Lyon, D.; Nesser, H.; Sulprizio, M. P.; Varon, D. J.; Zhang, R. Quantifying Methane Emissions from the Largest Oil-Producing Basin in the United States from Space. *Sci. Adv.* **2020**, *6* (17).eaaz5120

https://dx.doi.org/10.1021/acs.est.0c02927
Environ. Sci. Technol. 2020, 54, 13926−13934